Two New Layered Thioantimonate(III) Compounds: Solvothermal Syntheses, Crystal Structures, and Properties of (*trans*-1,4-$C_6N_2H_{15}$)Sb_3S_5 and (*trans*-1,2-$C_6N_2H_{15}$)$Sb_3S_5 \cdot H_2O$

Lars Engelke,[a] Christian Näther,[a] and Wolfgang Bensch*[a]

Keywords: Crystal structure / Hydrogen bonds / Solvothermal synthesis / Thioantimonate

Two new thioantimonate(III) compounds (*trans*-1,4-chxnH)Sb_3S_5 (**I**) and (*trans*-1,2-chxnH)$Sb_3S_5 \cdot H_2O$ (**II**) (chxn = diaminocyclohexane = $C_6N_2H_{14}$) were prepared under solvothermal conditions. Structure-directing arrangements of the organic molecules are formed under the conditions of synthesis; these consist of hydrogen-bonded chains (**I**) and of double chains of the amine molecules indirectly joined by water molecules through hydrogen bonding (**II**). In both compounds the structure-directing counter-ions are arranged in a layer-like fashion and because of the similar arrangements the topologies of the thioantimonate(III) layers $^2_\infty[Sb_3S_5]^-$ are nearly identical. The anionic layers are formed by interconnection of SbS_3 trigonal pyramids and SbS_4 moieties. The layers containing Sb_2S_2, Sb_4S_4, and $Sb_{10}S_{10}$ heterorings as secondary building units are stacked parallel to the *b* axis. The anionic layers and the structure-directing aggregates are stacked in a sandwich-like fashion. The water molecule in **II** can be removed at low temperatures, and this process is partially reversible. Interestingly, the removal of water is accompanied by a pronounced colour change from bright yellow to red.

(© Wiley-VCH Verlag GmbH, 69451 Weinheim, Germany, 2002)

Introduction

Structure-directing molecules such as alkylamines or their ammonium salts are widely used for the solvothermal synthesis of new main group thiometallates. A large number of thioantimonates(III) have been synthesized over recent years. The high flexibility of the coordination behaviour of the Sb^{III} atom, with coordination numbers between 3 and 6[1–4] due to the lone pair effect,[5,6] has allowed the preparation of a large variety of thioantimonate(III) compounds.

With alkali or alkaline metal cations, a size dependence of the anion dimensionality is observed. With decreasing ionic radius the formation of one-dimensional chains,[7] layered anions,[8] or three-dimensional networks[9] is preferred. In cases of transition metal amine complexes[10–12] or pure alkylammonium cations[13–15] no simple relationship between the size and the dimensionality of the thioantimonate(III) anion could be observed; thus, other factors must play a dominant role during the anionic framework formation. Systematic investigations are required in order to obtain a deeper knowledge of the factors influencing the formation and crystallization of thioantimonates(III). One approach to study the influence of the structure-directing molecules is the application of amines of similar size and charge but with their amino groups at different positions. Such an amine pair is *trans*-1,2-diaminocyclohexane and *trans*-1,4-diaminocyclohexane. In this contribution we report the syntheses, crystal structures, thermal stabilities, and optical properties of the two new thioantimonate(III) (chxnH)$[Sb_3S_5]$ species, with chxnH being the protonated amines *trans*-1,2-diaminocyclohexane and *trans*-1,4-diaminocyclohexane.

[a] Institut für Anorganische Chemie, Universität Kiel, Olshausenstr. 40, 24098 Kiel, Germany

Results and Discussion

Both (*trans*-1,4-chxnH)Sb_3S_5 (**I**) and (*trans*-1,2-chxnH)$Sb_3S_5 \cdot H_2O$ (**II**) crystallize in the triclinic space group $P\bar{1}$ with two formula units in the unit cell (Table 1). The Sb(1) and Sb(2) atoms in both **I** and **II** are coordinated by three sulfur atoms, forming the well-known SbS_3 pyramids. The Sb–S distances range from 2.396(1) to 2.5993(8) Å in **I** (Table 2) and from 2.393(1) to 2.599(1) Å in **II** (Table 3). In both compounds the Sb(3) atoms are coordinated by four S atoms to form an SbS_4 unit with two shorter Sb–S distances [2.4299(8) and 2.452(1) Å in **I** and 2.435(1) and 2.450(1) Å in **II**] and two significantly longer Sb–S separations [2.684(1) and 2.777(1) Å in **I** and 2.615(1) and 2.908(1) Å in **II**]. Such SbS_4 building units are common, and the two longer Sb–S distances are always in *trans* relationships to each other.[16–19] The coordination spheres of the antimony atoms are completed by S atoms at greater distances, giving coordination numbers of five [Sb–S: 2.978(1) to 3.546(1) and 2.973(1) to 3.519(1) Å, respectively]

to form distorted SbS_5 trigonal bipyramids (Table 4 and Figure 1).

The $Sb(1)S_3$ and $Sb(2)S_3$ pyramids each share a common corner with the $Sb(3)S_4$ moiety, yielding the $Sb_3S_5^-$ anion. Further interconnection to produce the two-dimensional

Table 1. Details of the data collections and some refinement results for the two compounds (*trans*-1,4-chxnH)Sb_3S_5 (**I**) and (*trans*-1,2-chxnH)Sb_3S_5 (**II**)

	(1,4-chxn)Sb_3S_5	(1,2-chxn)$Sb_3S_5{\cdot}H_2O$
a [Å]	6.713(1)	6.660(1)
b [Å]	10.059(2)	10.889(2)
c [Å]	12.368(3)	12.430(3)
α [°]	83.34(3)	105.43(3)
β [°]	84.15(3)	94.58(3)
γ [°]	73.13(3)	106.42(3)
V [Å^3]	791.7(3)	821.7(3)
Temperature [K]	293(2)	293(2)
Z	2	2
μ [mm^{-1}]	5.719	5.518
Formula mass [g/mol]	640.75	658.77
Space group	$P\bar{1}$	$P\bar{1}$
Density (calcd.) [g/cm^3]	2.688	2.663
Diffractometer	PHILIPS 4-circle	NONIUS CAD4
2Θ range [°]	3−60	4−60
Data collected	4991	5143
Unique data	4625	4763
Data [$F_o > 4\sigma(F_o)$]	4179	3874
Δρ [e/Å^3]	0.55/−0.67	1.06/−2.07
Refined parameters	206	183
y, z[a]	0.0244/0.28	0.0422/0.54
$R1[F_o > 4\sigma(F_o)]$	0.0177	0.0277
$wR2$ for all data	0.0455	0.0700
Goodness of fit	1.054	1.017

[a] $w = 1/[\sigma^2(F_o^2) + (yP)^2 + zP]$; $P = [\mathrm{Max}(F_o^2,0) + 2F_c^2]/3$.

Table 2. Distances [Å] and angles [°] in (*trans*-1,4-chxnH)Sb_3S_5 (**I**); estimated standard deviations are given in parentheses

Sb(1)−S(1)	2.419(1)	Sb(1)−S(1a)	2.5993(8)
Sb(1)−S(5)	2.460(1)	Sb(2)−S(2)	2.462(1)
Sb(2)−S(3)	2.396(1)	Sb(2)−S(4)	2.5812(8)
Sb(3)−S(2)	2.4299(8)	Sb(3)−S(3)	2.777(1)
Sb(3)−S(4)	2.452(1)	Sb(3)−S(5)	2.684(1)
Long contacts			
Sb(1)−S(2)	3.357(1)	Sb(1)−S(5a)	2.978(1)
Sb(2)−S(3a)	3.020(1)	Sb(2)−S(4a)	3.397(1)
Sb(3)−S(1)	3.546(1)		
S(1)−Sb(1)−S(1a)	88.79(2)	S(1)−Sb(1)−S(2)	80.17(1)
S(1)−Sb(1)−S(5)	95.12(2)	S(1a)−Sb(1)−S(5a)	82.44(1)
S(1a)−Sb(1)−S(2)	81.50(1)	S(1a)−Sb(1)−S(5)	100.47(2)
S(2)−Sb(1)−S(5a)	97.15(1)	S(5)−Sb(1)−S(5a)	87.80(1)
S(1a)−Sb(1)−S(5a)	171.13(2)	S(2)−Sb(1)−S(5)	174.90(1)
S(2)−Sb(2)−S(3a)	81.26(1)	S(2)−Sb(2)−S(3)	95.59(1)
S(2)−Sb(2)−S(4)	85.97(1)	S(3)−Sb(2)−S(4)	88.70(1)
S(3)−Sb(2)−S(3a)	87.42(1)	S(3)−Sb(2)−S(4a)	77.42(1)
S(3a)−Sb(2)−S(4)	95.59(1)	S(4)−Sb(2)−S(4a)	96.45(1)
S(2)−Sb(2)−S(4a)	172.50(1)	S(3a)−Sb(2)−S(4)	166.23(2)
S(1)−Sb(3)−S(2)	78.52(1)	S(1)−Sb(3)−S(3)	110.18(1)
S(1)−Sb(3)−S(5)	72.54(1)	S(2)−Sb(3)−S(3)	87.06(1)
S(2)−Sb(3)−S(4)	99.44(1)	S(2)−Sb(3)−S(5)	83.65(1)
S(3)−Sb(3)−S(4)	90.04(1)	S(4)−Sb(3)−S(5)	86.89(1)
S(1)−Sb(3)−S(4)	159.42(1)	S(3a)−Sb(3)−S(5)	169.59(1)

Table 3. Distances [Å] and angles [°] in (*trans*-1,2-chxnH)$Sb_3S_5{\cdot}H_2O$ **II**; estimated standard deviations are given in parentheses

Sb(1)−S(1)	2.415(1)	Sb(1)−S(1a)	2.524(1)
Sb(1)−S(5)	2.494(1)	Sb(2)−S(2)	2.485(1)
Sb(2)−S(3)	2.393(1)	Sb(2)−S(4)	2.599(1)
Sb(3)−S(2)	2.435(1)	Sb(3)−S(3)	2.908(1)
Sb(3)−S(4)	2.450(1)	Sb(3)−S(5)	2.615(1)
Long contacts			
Sb(1)−S(2)	3.385(1)	Sb(1)−S(5a)	3.139(2)
Sb(2)−S(3a)	2.973(1)	Sb(2)−S(4a)	3.519(1)
Sb(3)−S(1)	3.419(2)		
S(1)−Sb(1)−S(1a)	89.61(4)	S(1)−Sb(1)−S(2)	83.66(3)
S(1)−Sb(1)−S(5)	98.39(4)	S(1)−Sb(1)−S(5a)	79.97(4)
S(1a)−Sb(1)−S(2)	80.95(3)	S(1a)−Sb(1)−S(5)	97.20(4)
S(2)−Sb(1)−S(5a)	91.48(3)	S(5)−Sb(1)−S(5a)	90.68(3)
S(1a)−Sb(1)−S(5a)	167.78(4)	S(2)−Sb(1)−S(5)	177.25(3)
S(4)−Sb(2)−S(4a)	98.24(3)	S(2)−Sb(2)−S(4)	86.44(4)
S(3)−Sb(2)−S(4)	90.55(4)	S(3)−Sb(2)−S(4a)	77.64(3)
S(3a)−Sb(2)−S(4a)	91.49(3)	S(2)−Sb(2)−S(3)	97.74(4)
S(2)−Sb(2)−S(3a)	83.39(4)	S(3)−Sb(2)−S(3a)	85.69(4)
S(2)−Sb(2)−S(4a)	173.39(4)	S(3a)−Sb(2)−S(4)	168.58(4)
S(1)−Sb(3)−S(2)	81.43(3)	S(1)−Sb(3)−S(3)	103.69(3)
S(1)−Sb(3)−S(5)	74.69(3)	S(2)−Sb(3)−S(4)	98.33(4)
S(2)−Sb(3)−S(3)	85.67(4)	S(2)−Sb(3)−S(5)	86.27(4)
S(3)−Sb(3)−S(4)	90.18(4)	S(4)−Sb(3)−S(5)	91.36(4)
S(1)−Sb(3)−S(4)	166.04(3)	S(3a)−Sb(3)−S(5)	171.94(4)

Table 4. Differences [Å] for Sb−S bonds expressed as Δ(Sb−S in **II** − Sb−S in **I**)

Sb(1)−S(1)	−0.004	Sb(1)−S(1a)	−0.075
Sb(1)−S(5)	+0.034	Sb(2)−S(2)	+0.023
Sb(2)−S(3)	−0.003	Sb(2)−S(4)	+0.018
Sb(3)−S(2)	+0.005	Sb(3)−S(3)	+0.131
Sb(3)−S(4)	−0.002	Sb(3)−S(5)	−0.069
Long contacts			
Sb(1)−S(2)	+0.028	Sb(1)−S(5a)	+0.161
Sb(2)−S(3a)	−0.047	Sb(2)−S(4a)	+0.122
Sb(3)−S(1)	−0.127		

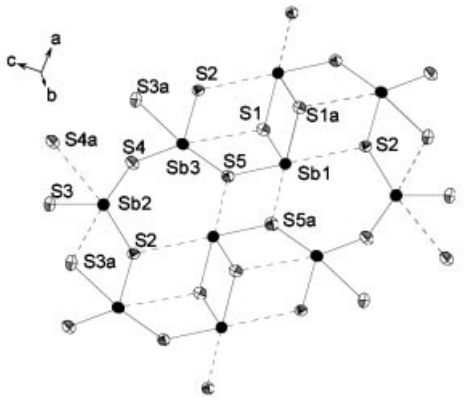

Figure 1. The environment of the Sb atoms, atom labelling and the long Sb−S contacts shown as dotted lines; the probability ellipsoids are drawn at the 50% level

layered anion is achieved by corner- and edge-sharing in the different primary building units. Two symmetry-related $Sb(1)S_3$ pyramids share a common edge to form a *trans*-Sb_2S_4 unit, and two $Sb(3)S_4$ and two $Sb(2)S_3$ have common corners, yielding a puckered, eight-membered Sb_4S_4 ring (8MR). The 8MR units are condensed into rods running along the *a* axis. Adjacent rods are connected by the *trans*-Sb_2S_4 building units, giving the two-dimensional $[Sb_3S_5]^-$ anion extending within the *a*−*c* plane shown in Figure 2. The connection of the rods by the Sb_2S_4 units gives rise to the formation of ellipsoidal 20-membered $Sb_{10}S_{10}$ heterorings (20MR) with approximate dimensions of 9.2×3 Å (measured from coordinate to coordinate). The layers are stacked perpendicular to the *b* axis (interlayer spacing about 6.9 Å) with a parallel alignment of the 8MR and 20MR units. The thickness of the individual layers is about 3.5 Å.

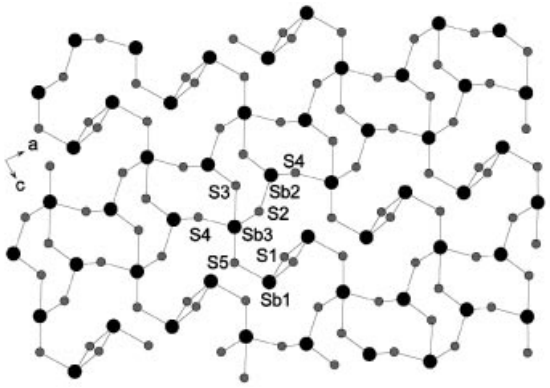

Figure 2. The $[Sb_3S_5^-]_\infty$ layer viewed parallel to [010], with numbering scheme and the four-, eight-, and 20-membered rings

In compound **I**, protonation of one of the two NH_2 groups yields the charge-balancing *trans*-1-amino-4-ammoniocyclohexane cation. Strong hydrogen bonds [N···H distance: 1.86(2) Å; N−H···N angle: 172.26(4)°] between adjacent cations (see Figure 3) force the arrangement of nearly linear chains running parallel to the *a* axis. The chains are oriented parallel to one another to form pseudo-layers within the *a*−*c* plane. As shown in Figure 4, the anionic Sb_3S_5 layers and cationic pseudo-layers are stacked in a sandwich-like manner perpendicular to the *b* axis.

Figure 3. Hydrogen bonds in the *trans*-1-amino-4-ammoniocyclohexane chains; the displacement ellipsoids are drawn at the 50% probability level

In compound **II**, one of the amino groups is again protonated to form the *trans*-1-amino-2-ammoniocyclohexane cation for charge-balancing. Hydrogen bonds between the

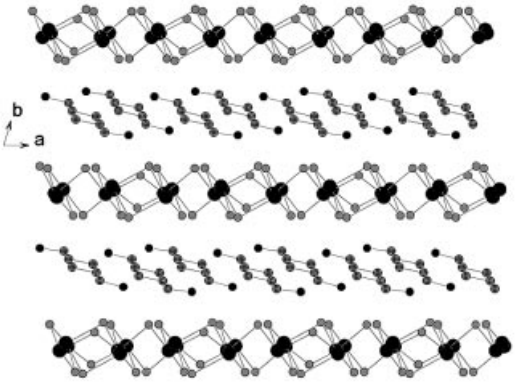

Figure 4. The sandwich-like arrangement of alternating anionic and cationic layers viewed along [001] in compound **I**

NH_2 and NH_3^+ groups in the 1- and 2-positions cannot give rise to the formation of linear chains as observed for the *trans*-1-amino-4-ammoniocyclohexane cation. In this compound, pairs of cations are formed, connected through hydrogen bonds involving two water molecules (Figure 5). The O···H distance of 1.85(5) Å and the N···H distance of 1.87(7) Å, with corresponding angles of 165.5° and 175.6°, are indicative of strong hydrogen bonds. An additional, weaker O···H hydrogen bond between the NH_3^+ groups and the water molecules interconnects the pairs to produce double chains. The O···H distance of 2.03(4) Å, the corresponding angle of 177.4°, and the N···O distance of 2.87(4) Å are common values for weaker hydrogen bonds.[20] The double chains running along the *a* axis are arranged in a layer-like fashion within the *a*−*c* plane. As in compound **I**, a sandwich-like structure consisting of alternating anionic and cationic layers stacked perpendicular to the *b* axis is observed. The differences between the arrangements of the cations in the two compounds are presumably due to the type of H bonding. In compound **I**, the amine molecules are joined by direct hydrogen bonds, whereas the connection in compound **II** involves a bridging water molecule. This acts as a donor and acceptor to two adjacent cations and is an acceptor for a third amine molecule.

At first glance, the two anionic network structures seem to be identical. However, a more detailed analysis reveals several differences, demonstrating the high flexibility of Sb^{III} coordination spheres for optimization of the packing (see Table 4). If only the short Sb−S bonds are taken into account, the average Sb−S distances of 2.526 Å (**I**) and 2.532 Å (**II**) are identical (Table 4). A small difference is observed when the long bonds are also considered [<Sb−S> = 2.771 Å for **I** and 2.783 Å for **II**]. The flexible behaviour can be demonstrated by comparing the environments of Sb(3) in the two compounds. In **I** the Sb(3)−S(3) and Sb(3)−S(5) separations are 2.777(1) Å and 2.684(1) Å, whereas in **II** these values amount to 2.908(1) Å and 2.615(1) Å. Because the bond order of the S(5) atom has to remain constant, the Sb(1)−S(5) bond in **I** [2.460(1) Å] is shorter than in **II** [2.494(1) Å].

Some remarkable differences are also observed for the S−Sb−S angles. In **I**, these values range from about 72.5

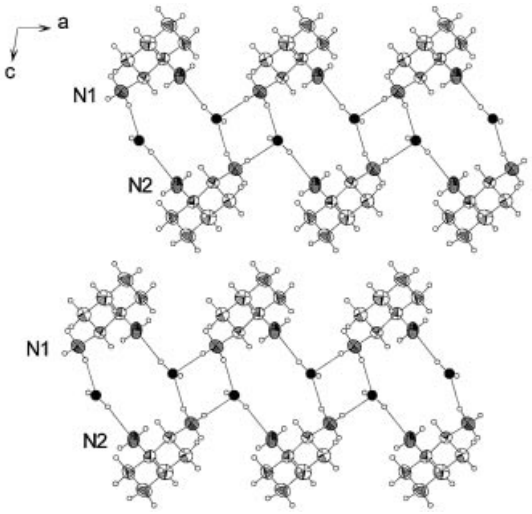

Figure 5. View of the *trans*-1-amino-2-ammoniocyclohexane cations and the water molecules forming double chains in the $a-c$ plane (displacement ellipsoids are drawn at the 50% probability level; hydrogen bonds are shown as dotted lines)

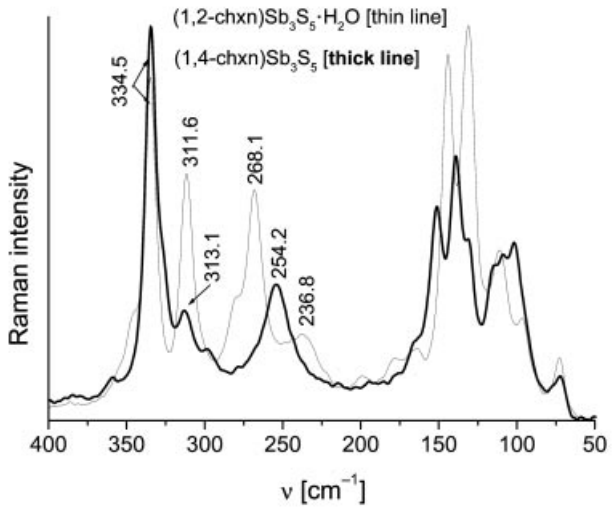

Figure 6. Raman spectra of (*trans*-1,4-chxnH)Sb_3S_5 and (*trans*-1,2-chxnH)$Sb_3S_5{\cdot}H_2O$; the numbers are the frequencies of some of the most intense resonances

to 110.2° whereas in **II** the analogous values extend from 74.7 to 103.7° (note: *trans*-S−Sb−S angles are not considered). Individual angles show differences of up to about 6.5° [S(1)−Sb(3)−S(3)], again demonstrating the flexibility of the thioantimonate(III) network for achievement of optimum packing.

As previously demonstrated, the bonding properties of a lone-pair atom are best detected from changes of the bond angles, whereas interatomic bond lengths are only slightly affected,[21] and the local environment of the Sb^{III} atoms exhibits no significant alterations of the Sb−S distances. Raman spectroscopy is a powerful tool for the detection of differing bonding properties; the Raman spectra are shown in Figure 6. Both compounds show intense bands located at 334.5 cm^{-1} (**I** and **II**) and at 313.1 cm^{-1} (**I**) or 311.6 cm^{-1} (**II**), due to SbS_3 and SbS_4 units.[22] Because of the similar average Sb−S bond lengths in **I** and **II**, the main resonances show only minute differences. However, small shoulders on the high-frequency side of the first band are caused by the different Sb environments in the two compounds. The assignments of the Sb−S modes are in accordance with the results reported by Pfitzner for Cu_3SbS_3 and $(CuI)_2Cu_3SbS_3$.[23] In the former compound, two maxima were observed at 321 and 290 cm^{-1}, reflecting the weaker bonding interaction due to the 3 + 5 environment. In the latter, the [SbS_3^{3-}] anion has no next-nearest S atoms, yielding Raman bands at 362 and 339 cm^{-1}. For $Mn_2Sb_2S_4$, with one Sb^{III} atom in a sixfold environment of S atoms and the other Sb^{III} atom in a sevenfold one, Raman bands occur at even lower frequencies, being located between about 280 and 310 cm^{-1}.[24]

A brief comparison of the crystal structures of **I** and **II** with structures of composition RSb_3Q_5 (R = cation, Q = S, Se) should serve to highlight the uniqueness of the thioantimonate(III) layers in the title compounds. In $RbSb_3S_5{\cdot}H_2O$[16] and $RbSb_3Se_5$,[25] layered anions are found. In these two compounds, however, remarkably different modes of interconnection of the primary building units to form SbS/SbSe heterorings are found. In the selenide, six- and eight-membered rings are formed, while in the sulfide the interconnection yields four- and 16-membered rings. Compounds $[M^{II}(en)_3]Sb_3S_5$ with M = Ni, Co[26] contain isolated $[Sb_3S_5]^-$ anions. With large organic cations such as Tpa [tetrapropylammonium, $(C_3H_7)_4N^+$] or PPh_4 (tetraphenylphosphonium), the SbS_x units are joined to form one-dimensional chains, as found in $(Tpa)Sb_3S_5$ [11] and $(PPh_4)Sb_3S_5$.[27] With the smaller Tma [tetramethylammonium, $(CH_3)_4N^+$] cation, three-dimensional interconnection of the primary units of the Sb_3S_5 anion was proposed.[28] The ternary compound $TlSb_3S_5$ [29] shows a three-dimensional anionic framework. We note that the two title compounds are the first examples of thioantimonate(III) moieties with $[Sb_3S_5]^-$ networks containing 4MR, 8MR, and 20MR components as secondary building units.

With respect to the syntheses of the compounds, several observations are remarkable. Compound **I** forms under a wide range of conditions, with factors such as temperature, amine concentration, and amine/antimony ratio having virtually no influence on product formation. Several unsuccessful attempts were made to introduce transition metal cations into the anionic thioantimonate(III) framework. In all experiments compound **I** was obtained. Hence, we conclude that, under the reaction conditions used, *trans*-1,4-diaminocyclohexane forms a very stable arrangement that forces the growth of $^2_\infty[Sb_3S_5]^-$ layers with the topology found in the title compound. In contrast, the synthesis of **II** requires very precise conditions, suggesting a lower stability of the hydrogen-bonded 1,2-substituted amine. Parameters such as temperature, amine concentration, and amine/antimony ratio were varied in a large number of experiments. Small deviations from the synthesis conditions reported in the Exp. Sect., though, always yield thioanti-

monates of different composition. In addition, application of Mn, Ni, or Co results in the formation of compounds composed of isolated $[M(chxn)_3]^{2+}$ and SbS_4^{3-} ions (M = Co, Ni) or of $[M(chxn)_2(SbS_4)_2]^{4-}$ ions (M = Mn). Obviously, the formation of the structure-directing arrangement of the cations requires precise conditions, and deviations from exact stoichiometric quantities suppress the "template" formation.

Thermal Investigations

The DTA-TG curves are shown in Figure 7. Compound **I** starts to decompose at T_{onset} = 250 °C. A weight loss of 18.9% occurs in one step, and is accompanied by an endothermic signal with a peak temperature T_p of 257 °C. The mass loss is in good agreement with that calculated for the emission of the amine molecules ($-\Delta m_{theo}$ = 17.98%). In the X-ray powder pattern of the decomposition product, the reflections of crystalline Sb_2S_3 as well as of elemental antimony are found. Obviously, the Sb/S ratio in the starting material (0.6) results in a partial reduction of Sb^{III} to elemental Sb and the formation of Sb_2S_3. A C,H,N analysis of the residue yields a very low contamination level of about 0.5%.

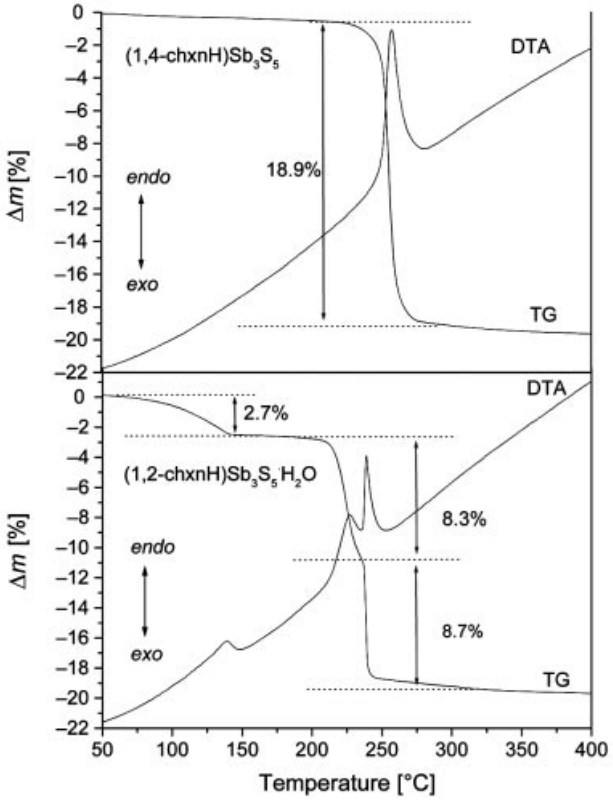

Figure 7. DTA/TG curves for compound **I** (top) and for compound **II** (bottom; mass changes are given in %)

For compound **II** the decomposition reaction is more complex. In the first step, a weight loss of 2.7% is observed at T_{onset} = 80 °C, accompanied by an endothermic signal at T_p = 139 °C. This weight change is in agreement with the emission of the water molecule ($-\Delta m_{theo}$ = 2.7%). On further heating, two strongly endothermic signals occur at T_{onset} = 220 and 230 °C, with DTA signals at T_p = 227 and 239 °C. The total weight loss is about 17.0%, suggesting successive decomposition of the amine. The experimental mass change is close to the value expected for the removal of the amine ($-\Delta m_{theo}$ = 17.4%). The X-ray powder pattern of the final product is identical with that obtained for the decomposition product of **I**.

In a further experiment, thermal decomposition was interrupted after the emission of the water molecule. The formerly yellow compound exhibited a significant darkening to red. The X-ray powder pattern shows a significant shift of the (0*k*0) reflections to larger 2θ values (see Figure 8), representing a reduction of the interlayer distance from 9.95 to 9.52 Å. The removal of H_2O is partly reversible, and the X-ray powder pattern after a few days in humid air is similar to that of the pristine material. The positions of the (010) and (020) reflections shifted to 2θ values very close to those determined for the original material. The alteration of the reflection profiles indicate that the process is not fully reversible. This is further supported by the orange colour of the sample, in comparison to the yellow colour of the pristine material.

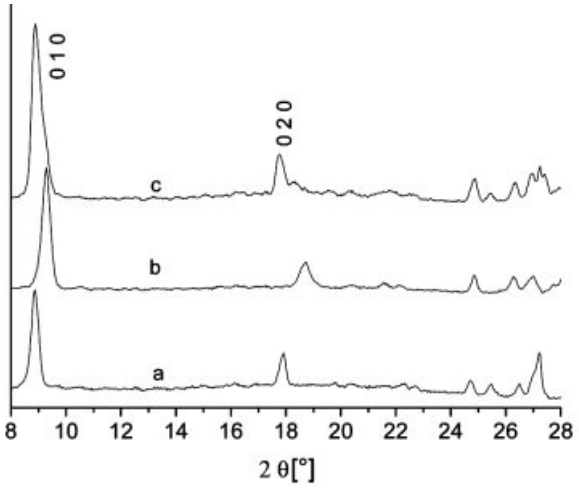

Figure 8. X-ray powder patterns of compound **II**: as prepared (a), after removal of water (b), and after treatment of the water-free sample in humid air (c); for two reflections the indices are given

Conclusion

The crystal structures of the two new thioantimonate(III) compounds are excellent examples demonstrating the structure-directing effect of the amines used under solvothermal conditions. The topologies of the $^2_\infty[Sb_3S_5]^-$ layers in **I** and **II** are very similar, but with some distinct differences demonstrating the high flexibility of Sb^{III} coordination spheres. The structure-directing cations are formed in situ, and the stability seems to be determined mainly by the location of the two amino functions. Compound **I** is formed under a wide range of reaction conditions, strong intermolecular hy-

drogen bonds resulting in the stable arrangement of the cations. In contrast, compound **II** is only formed in a very narrow window of reaction conditions, and water molecules are necessary for the formation of the structure-directing arrangement. The anionic layers and the structure directors are stacked in a sandwich-like manner. The removal of water from **II** is partially reversible and is accompanied by a significant change of the colour from bright yellow to red. We are currently investigating whether the uptake of other polar molecules into the water-free material is possible. In addition, the 1,3-diamino- and 1,3,5-triaminocyclohexane should be used in further solvothermal syntheses to provide information on the influence of the structure-directing molecules on product formation.

Experimental Section

Syntheses of (*trans*-1,4-chxnH)Sb_3S_5 (I) and (*trans*-1,2-chxnH)$Sb_3S_5 \cdot H_2O$ (II) (chxn = Diaminocyclohexane, $C_6H_{14}N_2$): The two compounds were prepared under solvothermal conditions in a Teflon-lined steel autoclave with an inner volume of 30 mL. For **I**, a mixture of elemental antimony (122 mg, 1 mmol) and sulfur (80 mg, 2.5 mmol) was heated with *trans*-1,4-diaminocyclohexane (0.65 g, 5.7 mmol) and water (2.5 mL) to 140 °C for 5 d. For **II**, the same amounts of Sb and S were applied, but a mixture of water (1.5 mL) and *trans*-1,2-diaminocyclohexane (1.5 mL, 12.5 mmol) was used (120 °C for 5 d). The products were filtered and washed with water and acetone. Single crystals suitable for X-ray investigations were obtained under static conditions. Pale yellow, air-stable platelets were obtained in yields of about 75% based on antimony. Both compounds could also be prepared whilst stirring. For **I**, a mixture of Sb (122 mg, 1 mmol), S (64 mg, 2 mmol), amine (0.8 g, 7 mmol), and water (2 mL) was heated in a Teflon-lined autoclave of 7 mL internal volume, while for **II**, the amine (1.5 mL, 12.5 mmol) was diluted with water (0.5 mL). When the slurry was stirred, the reactions were complete after 3 h, with yields of 90% based on antimony. The yellow microcrystalline powders were shown to be phase-pure by X-ray powder diffraction. **I:** (640.75): calcd. C 11.24, H 2.36, N 4.37; found C 11.06, H 2.29, N 4.30. **II:** (658.77): calcd. C 10.94, H 2.58, N 4.25; found C 10.70, H 2.51, N 4.18.

X-ray Crystallography: The intensity data were collected with PHILIPS PW1100 four-circle (**I**) and NONIUS CAD4 (**II**) diffractometers, with graphite-monochromated Mo-K_α radiation (λ = 0.71073 Å). The structures were solved by use of SHELXS-97[28] and structure refinements were done against F^2 with SHELXL-97.[29] All non-hydrogen atoms were refined with anisotropic displacement parameters. All H atoms in **I** and those bound to N and O in **II** were located in the difference Fourier maps and were refined with varying coordinates and varying isotropic displacement parameters. In compound **II**, the H atoms bound to carbon atoms were positioned with idealized geometries and refined with fixed isotropic displacement parameters by use of a riding model. The details of data acquisition and some refinement results are listed in Table 1, and atom distances and angles are listed in Tables 2−3. CCDC-178624 (**I**) and -178625 (**II**) contain the supplementary crystallographic data for this paper. These data can be obtained free of charge at www.ccdc.cam.ac.uk/conts/retrieving.html or from the Cambridge Crystallographic Data Centre, 12, Union Road, Cambridge CB2 1EZ, UK [Fax: (internat.) + 44-1223/336-033; E-mail: deposit@ccdc.cam.ac.uk].

X-ray Powder Diffraction: The X-ray powder patterns were recorded in transmission geometry with a STOE Stadi-P diffractometer with Cu-$K_{\alpha 1}$ radiation (λ = 1.540598 Å).

Thermal Analysis: The thermal investigations were performed with a Netzsch STA 429 DTA-TG device. The samples were heated in Al_2O_3 crucibles, with a heating rate of 3 °C min^{-1}, up to 600 °C and purged in an argon stream (approximately 100 mL min^{-1}). The data were corrected for buoyancy effects.

Raman Spectroscopy: The Raman spectra were measured from 50 to 3500 cm^{-1} with a Bruker IFS 66 Fourier transform Raman spectrometer (wavelength: 1064 nm).

Acknowledgments

This work was supported by the state of Schleswig-Holstein and the Fonds der Chemischen Industrie.

[1] W. S. Sheldrick, M. Wachold, *Angew. Chem. Int. Ed. Engl.* **1997**, *36*, 206−226.
[2] C. L. Cahill, B. Gugliotta, J. B. Parise, *Chem. Commun.* **1998**, 1715−1716.
[3] C. L. Bowes, G. A. Ozin, *Adv. Mater.* **1996**, *8*, 13−28.
[4] W. S. Sheldrick, M. Wachhold, *Coord. Chem. Rev.* **1998**, *176*, 211−322.
[5] C. L. Bowes, A. Lough, A. Malek, G. A. Ozin, S. Petrov, D. Young, *Chem. Ber.* **1996**, *129*, 283−287.
[6] W. S. Sheldrick, H. Braunbeck, *Z. Naturforsch.* **1990,** *45B*, 1643−1646.
[7] G. Cordier, H. Schäfer, C. Schwidetzky, *Z. Naturforsch.* **1984,** *39b*, 131−134.
[8] W. S. Sheldrick, H.-J. Häusler, *Z. Anorg. Allg. Chem.* **1988**, *557*, 105−111.
[9] H. A. Graf, H. Schäfer, *Z. Naturforsch.* **1972,** *27b*, 735−739.
[10] R. Stähler, C. Näther, W. Bensch, *Chem. Commun.* **2001**, 477−478.
[11] H.-O. Stephan, M. G. Kanatzidis, *Inorg. Chem.* **1997**, *36*, 6050−6057.
[12] W. Bensch, M. Schur, *Z. Naturforsch.* **1997,** *52b*, 405−409.
[13] J. B. Parise, Y. Ko, *Chem. Mater.* **1992**, *4*, 1446−1450.
[14] X. Wang, *Chem. Ber.* **1995**, *32*, 303−312.
[15] A. V. Powell, S. Boissière, A. Chippindale, *Chem. Mater.* **2000**, *12*, 182−187.
[16] B. Eisenmann, H. Schäfer, *Z. Naturforsch.*, **1979**, *34B*, 383−385.
[17] X. Wang, F. Liebau, *J. Solid State Chem.* **1994**, *111*, 385−389.
[18] G. Schimek, J. Kolis, *Inorg. Chem.* **1997**, *36*, 1689−1693.
[19] R. Stähler, C. Näther, W. Bensch, *Eur. J. Inorg. Chem.* **2001**, 3073−3078.
[20] R. Taylor, O. Kennard, *Acta Crystallogr., Sect. B* **1983**, *39*, 133−138.
[21] X. Wang, F. Liebau, *Acta Crystallogr., Sect. B* **1996**, *52*, 7−15.
[22] X. Wang, F. Liebau, *Z. Kristallogr.* **1996**, *211*, 437−439.
[23] A. Pfitzner, *Chem. Eur. J.* **1997**, *3*, 2032−2038.
[24] A. Pfitzner, D. Kurowski, *Z. Kristallogr.* **2000**, *215*, 373−376.
[25] H. Rijnberk, C. Näther, W. Bensch, *Monatsh. Chem.* **2000**, *131*, 721−726.
[26] J. B. Parise, *Science* **1991**, *291*, 293−294.
[27] M. Gostojic, W. Nowacki, P. Engel, *Z. Kristallogr.* **1982**, *159*, 217−224.
[28] G. M. Sheldrick, *SHELXS-97, Program for Crystal Structure Determination*, University of Göttingen, Germany, **1997**.
[29] G. M. Sheldrick, *SHELXL-97, Program for the Refinement of Crystal Structures*, University of Göttingen, Germany, **1997**.

Received May 3, 2002
[I02219]